



HAL
open science

Procedure for the bond graph construction of an optimal control problem.

Omar Mouhib, Bogdan Chereji, Wilfrid Marquis-Favre, Daniel Thomasset,
Jérôme Pousin, Martine Picq

► **To cite this version:**

Omar Mouhib, Bogdan Chereji, Wilfrid Marquis-Favre, Daniel Thomasset, Jérôme Pousin, et al.. Procedure for the bond graph construction of an optimal control problem.. 13th IFAC Workshop on Control Applications of Optimisation (CAO'06), Apr 2006, Cachan, France. hal-00403245

HAL Id: hal-00403245

<https://hal.science/hal-00403245>

Submitted on 4 Apr 2019

HAL is a multi-disciplinary open access archive for the deposit and dissemination of scientific research documents, whether they are published or not. The documents may come from teaching and research institutions in France or abroad, or from public or private research centers.

L'archive ouverte pluridisciplinaire **HAL**, est destinée au dépôt et à la diffusion de documents scientifiques de niveau recherche, publiés ou non, émanant des établissements d'enseignement et de recherche français ou étrangers, des laboratoires publics ou privés.

PROCEDURE FOR THE BOND GRAPH CONSTRUCTION OF AN OPTIMAL CONTROL PROBLEM *

Omar Mouhib ¹ , Bogdan Chereji ¹ , Wilfrid Marquis-Favre ¹
Daniel Thomasset ¹ , Jerome Pousin ² , Martine Picq ²

Institut National des sciences Appliquées de Lyon

(1) Laboratoire d'Automatique Industrielle

(2) Institut Camille Jordan

25, avenue Jean Capelle, F-69621 Villeurbanne Cedex

e-mail: <firstname> .<lastname>@insa-lyon.fr

Abstract: This paper aims at providing a procedure and the proof of its effectiveness introducing an optimal control formulation into the bond graph language. The class of optimal control problems presented concerns linear time invariant MIMO systems where the integral performance index corresponds to minimising the input and dissipative energy. The procedure enables the formulation to be set up exclusively at a graphical (namely bond graph) level. The proof uses the Pontryagin principle applied to the port-Hamiltonian formulation of the system.

Keywords: Optimal control, bond graph, pontryagin Maximum Principle, port-hamiltonian system, bicausality.

1. INTRODUCTION

Dynamic optimisation involves systems where the variables are functions of time and where the models are governed by Differential- (either Ordinary or Algebraic) Equations (Pun, 1969),(Naidu, 2003). Also in many optimisation problems, the performance index is energy and/or state based. Thus it is justified to raise the question: "to what extent bond graph language, that straightforwardly displays both the dynamics and the energy topology of a system model, can be used to represent the formulation of an optimisation problem?". In the bond graph language context, work handling optimisation has principally a sensitivity approach (Cabanellas, 1999),(Roe, 2000),(Gawthrop, 2000b). Introducing optimisation into bond graph language brings a new vision on optimisation as can be experienced through this paper. Moreover coupling optimisation and bond graph has also System Engineering arguments. In fact a perspective is to extend a methodology for mechatronic system sizing on dynamic and energy criteria (Fotsu-Ngwompo, 2001),(Fotsu-Ngwompo, 1999). With this in view, the integration of actuating line component specifications, optimal con-

trol, multivariable control, energy minimization in the context of sustainable development, design specifications not precisely defined, structure synthesis is expected. Optimal control is the first step in this perspective of introducing a more general optimisation into bond graph language and a conjectural procedure has been recently proposed (Marquis-Favre, 2005). The proposed procedure concerns the optimal control of linear time invariant MIMO systems dealing with the Pontryagin Maximum Principle where the integral performance index is based on inputs and dissipation energy. Several approaches exist to deal with this category of optimisation problem and to furnish the analytical system with equations giving the optimal control solution. So the main contribution of this present work is to provide a new way based on the bond graph tool to formulate this analytical system. Boundary conditions are considered as fixed, in particular for both final time and final state and finally no constraint exists on inputs or states. This voluntary restricted hypothesis framework is the first step in coupling optimisation and bond graph which has been clearly investigated. It offers encouraging perspectives for future work.

The next section proposes a procedure for building the bond graph representation corresponding to the given optimal control problem. Section 3 demonstrates former procedure and prove its effectiveness. The key

* Acknowledgement: this work has been carried out within the scope of the RNTL-METISSE project and authorised by the French Ministry of National Education and Research

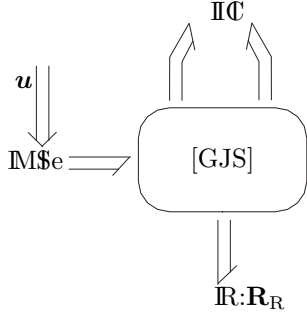


Fig. 1. Model bond graph

idea of the proof is to apply the Pontryagin Maximum Principle to a generic port-Hamiltonian system. Then the proposed procedure is shown in section 4 using the example of the DC motor example. Finally a conclusion and some perspectives are given in section 5.

2. PROCEDURE FOR THE BOND GRAPH FORMULATION OF AN OPTIMAL CONTROL PROBLEM

Proposition: *Given a linear time invariant model of a MIMO system with its bond graph representation (Fig. 1) and subject to an optimal control problem with input and dissipation-based integral performance index of the form (1) and with given boundary conditions; a bond graph representation furnishing, by bicausal exploitation, the set of differential-algebraic equations that analytically give the solution to the optimal control problem is shown in Fig. 2 where the junction structure and the multiport IC-element are identical.*

$$V = \int_{t_0}^{t_f} \frac{1}{2} (\mathbf{u}^T \cdot \mathbf{R}_u^{-1} \cdot \mathbf{u} + P_{\text{diss}}) dt \quad (1)$$

where \mathbf{R}_u is the control weighted matrix, \mathbf{I} is the identity matrix, P_{diss} is the dissipation power expressed as the inner product of the power conjugate vectors of the R-elements ($P_{\text{diss}} = \mathbf{e}_R^T \cdot \mathbf{f}_R$). Also a multiport graph notation has been adopted (Breedveld, 1986). In this notation GJS stands for Generalized Junction Structure.

Procedure:

- (1) For each control to be optimally determined, add to the model bond graph a R-element characterized by the factor of the square input term in the performance index. This R-element is connected to a junction inserted onto the control source bond and corresponding to the control variable nature i.e. a 0 (resp. 1)-junction for an effort (resp. flow). The added R-element may find its physical interpretation in some dissipative phenomenon of a non-ideal energy supply.
- (2) Duplicate the model bond graph with its parameters except for the R-elements. For the R-elements corresponding to the model dissipation phenomena, the characteristic matrices are transposed and

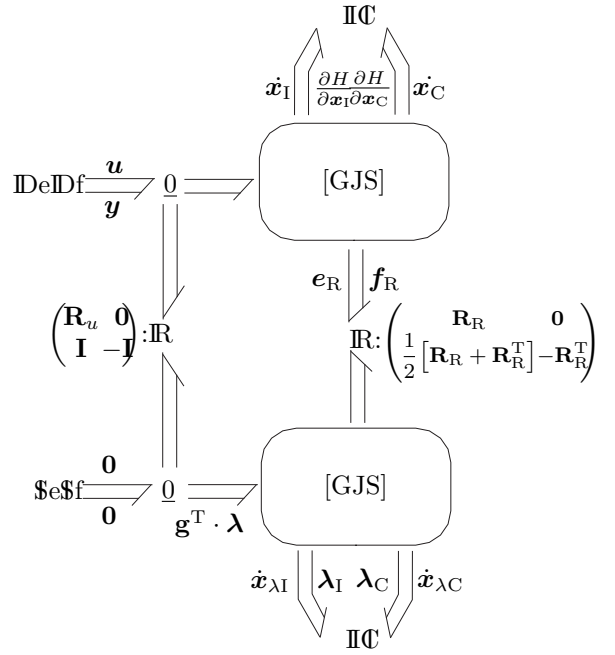


Fig. 2. Generic bond graph representation of an optimal control problem

sign reversed. For the R-elements added at step 1, the characteristic matrices are the negative identity matrices. In the case of 1-port R-elements, this simply corresponds to reversing the characteristic parameter sign or setting the parameter to 1. The duplicated representation is hereafter called *optimizing bond graph*.

- (3) For each dissipative phenomenon involved in the given integral performance index, couple the corresponding R-elements respectively in the model and the *optimizing* bond graphs by adding the matrix $\frac{1}{2} [\mathbf{R}_R + \mathbf{R}_R^T]$ as the lower extra diagonal submatrix. In the case of 1-port R-elements, the lower extra diagonal matrix coefficient is simply the model R-element parameter.
- (4) For each control to be optimally determine, couple the corresponding R-elements respectively in the model and *optimizing* bond graphs by adding the identity matrix as the lower extra diagonal submatrix. In the case of 1-port R-elements, this simply corresponds to adding 1.
- (5) Replace in the model bond graph the source elements involved in the optimal controls by double detectors and mirror them by double sources at the same place on the *optimizing bond graph*. The double sources impose both null efforts and flows.
- (6) Assign bicausality to the obtained bond graph. Bicausality propagates from the double sources to the double detectors and through the R-elements added at step 1. The analytical exploitation of the bicausal bond graph representation obtained provides the system equations and the optimal control solutions to the initial given problem.

3. PROOF OF THE EFFECTIVENESS OF THE PROCEDURE

This section proves that the bond graph representation obtained by the above procedure corresponds well to the given optimal control problem. The proof is based on the port-Hamiltonian system concept (Maschke, 1992),(Van der Schaft, 2001) that has been proven to be the geometric counterpart of the graphical bond graph representation.

Port-Hamiltonian system

Consider a system with the total stored energy represented by its Hamiltonian $H(\mathbf{x})$ expressed in this case as a quadratic form of \mathbf{x} (equation 2):

$$H(\mathbf{x}) = \frac{1}{2} \mathbf{x}^T \cdot \mathbf{H} \cdot \mathbf{x} \quad (2)$$

where the Hessian matrix \mathbf{H} is symmetric and definite positive. The port-Hamiltonian model with the hypothesis framework of a linear time-invariant system is given by (3) (Van der Schaft, 2001).

$$\begin{cases} \dot{\mathbf{x}} = [\mathbf{J} - \mathbf{S}] \cdot \frac{\partial H(\mathbf{x})}{\partial \mathbf{x}} + \mathbf{g} \cdot \mathbf{u} \\ \mathbf{y} = \mathbf{g}^T \cdot \frac{\partial H(\mathbf{x})}{\partial \mathbf{x}} \end{cases} \quad (3)$$

where \mathbf{J} and \mathbf{g} are constant matrices associated to junction structure transformations in the bond graph, \mathbf{S} is a constant matrix related to the dissipation phenomena and introduced hereafter, \mathbf{u} and \mathbf{y} are respectively the system input and output vectors. A canonical bond graph representation of equation (3) is given on Fig. 1 where $\mathbf{x} = [\mathbf{x}_C \ \mathbf{x}_I]$ (Karnopp, 2000). Also, by introducing the power conjugate variables \mathbf{e}_R and \mathbf{f}_R on the R-element ports (equations 4 and 5), the matrix \mathbf{S} may be decomposed as the equation (6) shows :

$$\mathbf{e}_R = \mathbf{R}_R \cdot \mathbf{f}_R \quad (4)$$

$$\mathbf{f}_R = \mathbf{g}_R^T \cdot \frac{\partial H(\mathbf{x})}{\partial \mathbf{x}} = \mathbf{g}_R^T \cdot \mathbf{H} \cdot \mathbf{x} \quad (5)$$

$$\mathbf{S} = \mathbf{g}_R \cdot \mathbf{R}_R \cdot \mathbf{g}_R^T \quad (6)$$

Where \mathbf{g}_R is a matrix associated to the junction structure transformation between the storage and the R-elements.

Application of the Pontryagin Maximum Principle on the port-Hamiltonian system

We consider the integral performance index in the form of some energy dissipation and input minimization:

$$V = \int_{t_0}^{t_f} \frac{1}{2} (\mathbf{u}^T \cdot \mathbf{R}_u^{-1} \cdot \mathbf{u} + P_{\text{diss}}) dt \quad (7)$$

The bond graph implementation of the control weighted matrix is displayed in Fig. 3. The Pontryagin function applied to the port-Hamiltonian system (3) with the equation (4) and the integral performance index (7) gives:

$$H_p = \frac{1}{2} \mathbf{u}^T \cdot \mathbf{R}_u^{-1} \cdot \mathbf{u} + \frac{1}{2} \mathbf{f}_R^T \cdot \mathbf{R}_R \cdot \mathbf{f}_R + \boldsymbol{\lambda}^T \cdot [\mathbf{J} - \mathbf{S}] \cdot \mathbf{H} \cdot \mathbf{x} + \mathbf{g} \cdot \mathbf{u} \quad (8)$$

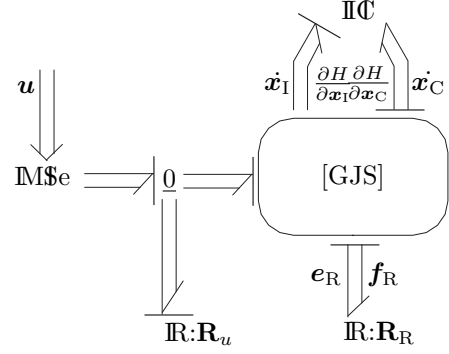


Fig. 3. Canonical bond graph representation for a port-Hamiltonian system

where $\boldsymbol{\lambda}$ is the vector of co-state variables usually called Lagrange multipliers of the associated constrained variational problem. The set of differential-algebraic equations (9) provides the optimal solution for \mathbf{x} , $\boldsymbol{\lambda}$ and \mathbf{u}

$$\begin{cases} \dot{\mathbf{x}} = \frac{\partial H_p(\mathbf{x}, \boldsymbol{\lambda}, \mathbf{u})}{\partial \mathbf{x}} \\ \dot{\boldsymbol{\lambda}} = -\frac{\partial H_p(\mathbf{x}, \boldsymbol{\lambda}, \mathbf{u})}{\partial \boldsymbol{\lambda}} \\ \frac{\partial H_p(\mathbf{x}, \boldsymbol{\lambda}, \mathbf{u})}{\partial \mathbf{u}} = 0 \end{cases} \quad (9)$$

We obtain:

$$\dot{\mathbf{x}} = [\mathbf{J} - \mathbf{S}] \cdot \mathbf{H} \cdot \mathbf{x} + \mathbf{g} \cdot \mathbf{u} \quad (10)$$

$$\dot{\boldsymbol{\lambda}} = -\mathbf{H} \cdot \mathbf{g}_R \cdot \frac{1}{2} [\mathbf{R}_R + \mathbf{R}_R^T] \cdot \mathbf{f}_R + \mathbf{H} \cdot [\mathbf{J} + \mathbf{g}_R \cdot \mathbf{R}_R^T \cdot \mathbf{g}_R^T] \cdot \boldsymbol{\lambda} \quad (11)$$

$$\mathbf{R}_u^{-1} \cdot \mathbf{u} + [\boldsymbol{\lambda}^T \cdot \mathbf{g}]^T = 0 \quad (12)$$

While equation (10) can be derived from the Fig. 3 bond graph representation, the key issue of the bond graph formulation of an optimal control problem resides in the translation of equations (11) and (12) into this language.

Before introducing the bond graph translation of this equation, the variable mapping $\mathbf{x}_\lambda = \mathbf{H}^{-1} \cdot \boldsymbol{\lambda}$ is carried out. This gives :

$$\dot{\mathbf{x}}_\lambda = \boldsymbol{\Lambda}_x + \boldsymbol{\Lambda}_\lambda \quad (13)$$

with $\boldsymbol{\Lambda}_x = -\mathbf{g}_R \cdot \frac{1}{2} [\mathbf{R}_R + \mathbf{R}_R^T] \cdot \mathbf{f}_R$ and $\boldsymbol{\Lambda}_\lambda = [\mathbf{J} + \mathbf{g}_R \cdot \mathbf{R}_R^T \cdot \mathbf{g}_R^T] \cdot \mathbf{H} \cdot \mathbf{x}_\lambda$.

The reason for this variable mapping is that the co-state vector $\boldsymbol{\lambda}$ is analog to co-energy variables in bond graph language while the vector \mathbf{x}_λ is analog to the energy variables. It is not difficult to see that $\boldsymbol{\Lambda}_\lambda$ is closely analog to the expression of the state equations as the equation (14) shows.

$$\mathbf{x} : [\mathbf{J} - \mathbf{g}_R \cdot \mathbf{R}_R \cdot \mathbf{g}_R^T] \cdot \mathbf{H} \longrightarrow \mathbf{x}_\lambda : [\mathbf{J} - \mathbf{g}_R \cdot (-\mathbf{R}_R^T) \cdot \mathbf{g}_R^T] \cdot \mathbf{H} \quad (14)$$

In consequence the Fig. 3 bond graph structure concerning the multiport storage element, the multiport R-element, and the junction structure between those two can be reproduced to represent the term $\boldsymbol{\Lambda}_\lambda$ contributing for $\dot{\mathbf{x}}_\lambda$ (Fig. 4). Inspection of the term $\boldsymbol{\Lambda}_x$ in equation (13) shows that its contribution stems from

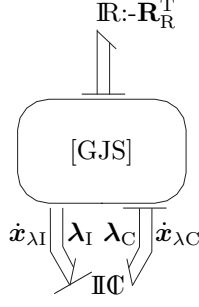


Fig. 4. Bond graph translation of the term Λ_λ contribution in equation (13)

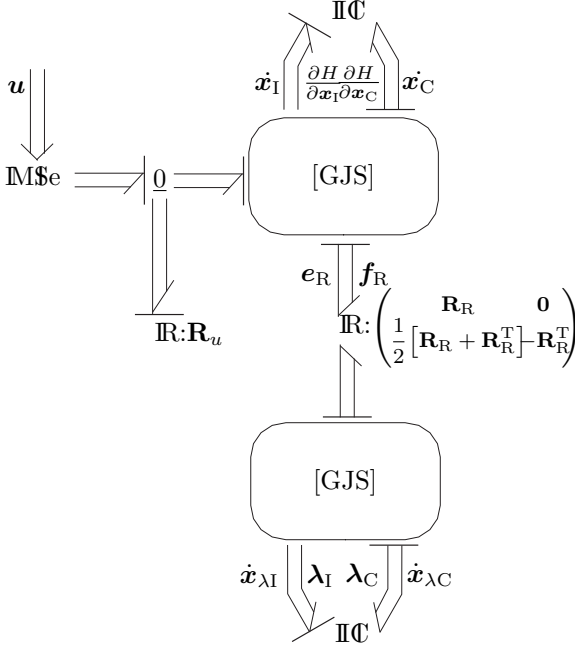


Fig. 5. Bond graph translation of both state and *optimizing-state* equations (10) and (13)

the previously introduced multiport R-element through the junction structure transformation characterized by \mathbf{g}_R . It results in the figure 5 bond graph translation that is a concatenation of the Fig. 3 and 4 bond graphs where the multiport R-elements have been replaced by a global multiport R-element characterized by the two matrices \mathbf{R}_R and $-\mathbf{R}_R^T$ arranged in block diagonal submatrices, and by the complementary lower extra diagonal submatrix $\frac{1}{2}[\mathbf{R}_R + \mathbf{R}_R^T]$. This multiport R-element represents the coupling between the state and *optimizing-state* equations. It has been proposed to call *optimizing-bond graph* the added bond graph representation mirroring to some extent the initial one. It remains now to treat equation (12) which corresponds to the Euler equation with respect to the control vector \mathbf{u} . First it is re-written as follows:

$$\mathbf{R}_u^{-1} \cdot \mathbf{u} + \mathbf{g}^T \cdot \boldsymbol{\lambda} = \mathbf{0} \quad (15)$$

This equation can be interpreted as an effort vector balance between a vector stemming from the control vector \mathbf{u} in the original system and a vector coming from the vector $\boldsymbol{\lambda}$ through the junction structure char-

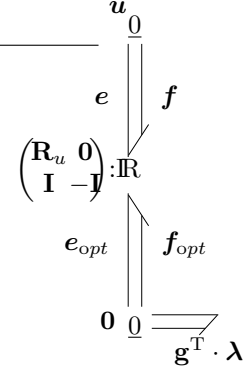


Fig. 6. Bond graph translation of Euler equation with respect to \mathbf{u} (12)

acterized by \mathbf{g} . This balance is translated by mirroring in the *optimizing bond graph* the part of the model bond graph located between the 0-junction array and the energy supply source (figure 6) and likewise by a concatenation of the multiport R-elements into a global multiport R-element characterized by the matrix (16).

$$\begin{pmatrix} \mathbf{R}_u & \mathbf{0} \\ \mathbf{I} & -\mathbf{I} \end{pmatrix} \quad (16)$$

Now by imposing simultaneously the null 2-flow vector balance and a null effort vector on the *optimizing bond graph* 0-junction array (figure 6), the Euler equations with respect to the \mathbf{u} components (12) are verified, as the following development proves, using the vector notations of figure 6:

from the second vector characteristic of the R-element:

$$\mathbf{e}_{opt} = \mathbf{f} - \mathbf{f}_{opt}$$

from the null effort vector balance:

$$\mathbf{f}_{opt} = -\mathbf{g}^T \cdot \boldsymbol{\lambda}$$

from the first vector characteristic of the R-element:

$$\mathbf{f} = \mathbf{R}_u^{-1} \cdot \mathbf{e} = \mathbf{R}_u^{-1} \cdot \mathbf{u}$$

then:

$$\mathbf{R}_u^{-1} \cdot \mathbf{u} + \mathbf{g}^T \cdot \boldsymbol{\lambda} = \mathbf{0}$$

It is thus justified not to have calculated the optimal controls *a priori* from the Euler equations in terms of the vector \mathbf{u} components. Finally The bond graph element that enables both a null effort vector and a 2-flow vector balance to be imposed on a 0-junction array is a multiport double source null effort vector and null flow vector. It is connected to the 0-junction array of the figure 6 bond graph. Such an element initializes a bicausality (Gawthrop, 2000a) propagation in the bond graph and thus requires the presence likewise of a multiport double detector (Fotsu-Ngwompo, 2001),(Fotsu-Ngwompo, 1999). In the mathematical formulation of the optimal control design problem, the role of the control vector \mathbf{u} is changed into an output vector and the power conjugate vector \mathbf{y} keeps its output vector role. In this way the multiport double detector replaces the original multiport MSe element in the figure 3 bond graph.

The final generic bond graph representation of the given optimal control problem is thus obtained (fig. 2).

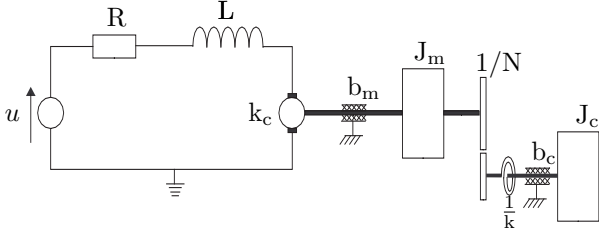


Fig. 7. DC motor model

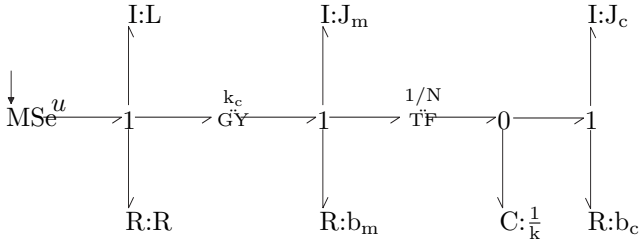


Fig. 8. DC motor bond graph representation

4. ILLUSTRATIVE EXAMPLE: THE DC MOTOR

This example illustrates a case where not all the dissipation energy is included in the integral performance index. The DC motor model is presented on Fig. 7. It consists of the armature electrical circuit composed of a voltage source u , a resistance R and an inductance L . The electromechanical coupling is characterized by the torque constant k . On the mechanical side the following items are considered: the rotor inertia J_m , a viscous friction on rotor (parameter b_m), a reduction gear (parameter $1/N$) with stiffness $\frac{1}{k}$, the load inertia J_c and a viscous friction on load shaft (parameter b_c). The model is linear and in the optimal control context, with the given initial conditions at t_0 and the final conditions at t_f , we aim at determining u with the integral performance index (17) that corresponds to the input and some dissipative energy minimization.

$$V = \int_{t_0}^{t_f} \frac{1}{2} \left(\frac{u^2}{R_u} + P_R + P_{b_c} \right) dt \quad (17)$$

where R_u is a control weighted factor, P_R is the electrical power dissipation and P_{b_c} is the power dissipation on the load shaft.

The bond graph representation of this DC motor model is given on Fig. 8. It shows the MSe element for the voltage source, three I-elements for the three energy storage phenomena respectively associated to the magnetic energy, and kinetic energies of the rotor and of the load shaft, a C-element for the energy storage associated to the reduction gear stiffness, and three R-elements for the dissipation phenomena respectively in the electrical circuit, on the rotor and on the load shaft. The GY-element represents the electro-mechanical coupling and the TF-element is associated to the power conserving coupling in the ideal reduction gear.

The equation (17) performance index involves the left-hand and right-hand side R-elements.

The section 2 procedure application for the five first steps provides the Fig. 9 bond graph representation. The bicausality assignment as shown on Fig. 9 bond graph, enables the optimal control system (18) to be obtained. This constitutes the final step of the section 2 procedure.

$$\begin{cases} \dot{p}_1 = -\frac{R}{L}p_1 - \frac{k_c}{J_m}p_2 - \frac{R_u}{L}p_{\lambda_1} \\ \dot{p}_2 = \frac{k_c}{L}p_1 - \frac{b_m}{J_m}p_2 - \frac{1}{kN}q_3 \\ \dot{q}_3 = \frac{1}{J_m N}p_2 - \frac{1}{J_c}p_4 \\ \dot{p}_4 = \frac{1}{k}q_3 - \frac{b_c}{J_c}p_4 \\ \dot{p}_{\lambda_1} = -\frac{R}{L}p_1 + \frac{R}{L}p_{\lambda_1} - \frac{k_c}{J_m}p_{\lambda_2} \\ \dot{p}_{\lambda_2} = \frac{k_c}{L}p_{\lambda_1} + \frac{b_m}{J_m}p_{\lambda_2} - \frac{1}{kN}q_{\lambda_3} \\ \dot{q}_{\lambda_3} = \frac{1}{J_m N}p_{\lambda_2} - \frac{1}{J_c}p_{\lambda_4} \\ \dot{p}_{\lambda_4} = -\frac{b_c}{J_c}p_4 + \frac{1}{k}q_{\lambda_3} + \frac{b_c}{J_c}p_{\lambda_4} \\ u = -\frac{R_u}{L}p_{\lambda_1} \\ y = \frac{1}{L}p_1 - \frac{1}{L}p_{\lambda_1} \end{cases} \quad (18)$$

The application of the Pontryagin Maximum Principle leads to the same result but with analytical developments compared to the bond graph graphical approach for deriving the equations.

Remark: The procedure proposed remains valid when the canonical bond graph contains multiport flow sources thus the add R-element on the flow control variable will be connected to a 1-connection. Also for the case where there are some R-elements with resistance causality and others with conductance causality, a partial dualisation can be used (Breedveld, 1985) with the help of symplectic gyrators that inverse the effort and

flow roles. thus we can Replace $\begin{bmatrix} \mathbf{R}_R & \mathbf{0} \\ \frac{1}{2} [\mathbf{R}_R + \mathbf{R}_R^T] & -\mathbf{R}_R^T \end{bmatrix}$

in optimal control bond graph with $\begin{bmatrix} \mathbf{R} & \mathbf{0} \\ \frac{1}{2} [\mathbf{R} + \mathbf{T}] & -\mathbf{R}^T \end{bmatrix}$

where \mathbf{R} (with $\mathbf{R} = \begin{bmatrix} \mathbf{R}_{rr} & \mathbf{R}_{rc} \\ \mathbf{R}_{cr} & \mathbf{R}_{cc} \end{bmatrix}$, r (resp. c) corresponding to a R-element port in resistance (resp. conductance) causality when bond graph is in integral causality) is the characteristic matrix of the corresponding model bond graph R-element and $\mathbf{T} = \begin{bmatrix} \mathbf{R}_{rr}^T & -\mathbf{R}_{cr}^T \\ -\mathbf{R}_{rc}^T & \mathbf{R}_{cc}^T \end{bmatrix}$.

5. CONCLUSION

The main contribution of this paper is to provide an alternative way for deriving an optimal control system for the kind of optimisation problem specified. Here the result is purely analytical and no method has been given for solving the equations of the system obtained. The corresponding approach is thus indirect

